Physics

Nuclear Physics

M. Sc. (Sem. - IV) (PHCT - 241) (Paper-I)

◆ Dr. R. B. Bhise ◆ Dr. M. D. Dhiware ◆ Prof. H. S. Shirke

◆ Prof. N. S. Sangle ◆ Prof. P. V. Darade

Choice Based Credit System (CBCS)

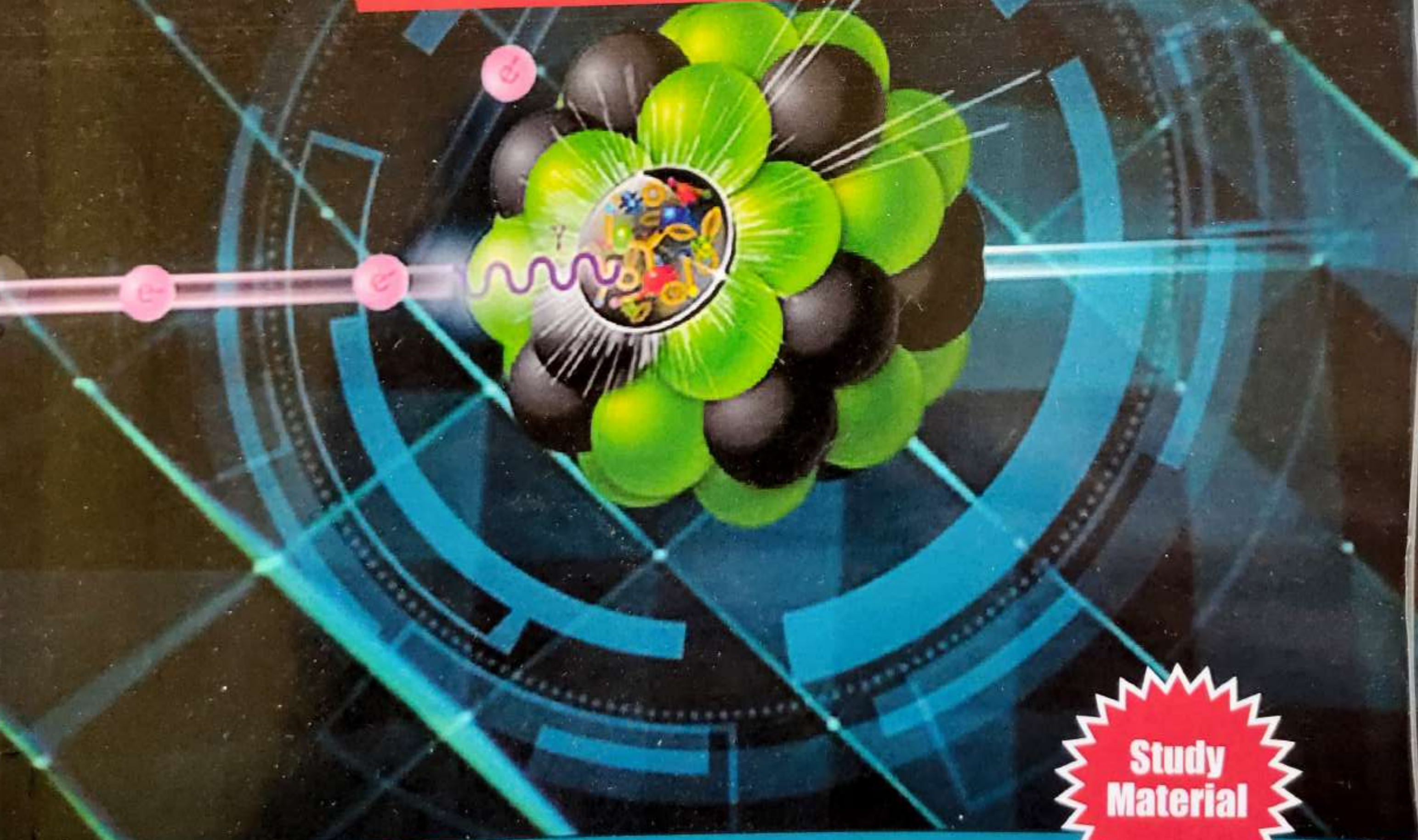

Study Material

SUCCESS PUBLICATIONS

Nuclear Physics

(PHCT-241)

M. Sc. (Sem. - IV) (Paper-I)

(According to New Syllabus of Savitribai Phule Pune University from June 2021)

Authors

Dr. Ramesh B. Bhise
(M.Sc., M.Phil., MBA., DCM, DIT, Ph.D.)
Head
Department of Physics
B. J. A. C. S. College, Ale Tal: Junnar, Dist: Pune.

Dr. Manisha D. Dhiware
(M.Sc., B.Ed., NET., Ph.D.)
Assistant Professor
Department of Physics,
K. V. N. Naik College, Nashik.

Prof. Hemant S. Shirke
(M.Sc., SET.)
Assistant Professor
Department of Physics
Annasaheb Awate College, Manchar, Pune.

Prof. Nandkishor S. Sangle
(M.Sc., SET.)
Assistant Professor
Department of Physics
K. V. N. Naik College, Nashik.

Prof. Pratik V. Darade
(M.Sc., B.Ed.)
Assistant Professor
Department of Physics
K. V. N. Naik College, Nashik.

2023

Price : 210/-

SUCCESS PUBLICATIONS

INDEX

M.Sc. (Sem. - IV) (Paper I)
Physics (Nuclear Physics) (PHCT-241)

Radiation Detectors and Nuclear Models

UNIT 2

2.1 Introduction :

If we perform any nuclear physics related experiment, nuclear radiation detectors play vital role in such measurements. Nuclear radiation is a general term and it includes a variety of energetic particles like electrons, protons, α-particles, heavy ions or neutral radiations like neutrons, X-rays or γ-rays etc. The development of radiation detectors started with the discovery of radioactivity by Henry Becquerel in 1896. He noticed that the radiations emitted by uranium salts blacken photosensitive paper. So, the first radiation detector was a photosensitive paper or X-ray film and was extremely simple. In the beginning of twentieth century, Rutherford used flashes of light produced in ZnS as nuclear radiation detector. These simple detectors used at that time were very primitive. They could simply indicate the presence or absence of radiations. Nowadays, it is not sufficient only to detect the presence or absence of radiations but one could also like to know the nature of radiations, i.e. whether the radiations are electrons, protons, α-particles, X-rays or γ-rays etc. On top of that, accurate energy and momentum measurements are often required. In some applications an exact knowledge of the spatial coordinates of the particle trajectories is also of interest.

Further, we will discuss some nuclear models in detail. We know that the size of nucleus is very small and nuclear forces are more complicated than other well-known forces. In fact, the picture of nuclear forces is still not clear. In order to understand and predict the properties of the nucleus, we have to know forces completely. For knowing nuclear forces, we adopt different approach. In nuclei, we choose an oversimplified theory, the treatment which is mathematically possible, but theory should be rich in physics. If this theory is fairly successful in accounting for at least a few properties of the nucleus, we can then improve the model by adding additional terms so that it is capable to account more nuclear properties. So, due to the lack of detailed knowledge of nuclear forces, nuclear models, namely liquid drop model, shell model, Fermi gas model, collective model, etc. have been developed.

2.2 Detectors :

In the field of nuclear instruments, "a detector is defined as a device which converts the energy of nuclear particle or radiation into a usable electric signal." An ideal detector would be able to differentiate between various types of radiation and particles and would give a signal which is proportional to their energy. In the study of petroleum, geology, cosmic rays, reaction rate, molecular structure, surface properties, equilibrium measurements and catalysis the nuclear detectors have found a use.

2.2.1 NaI (TI) Scintillation Detector :

It is a device which is used to detect and measure the radiations like protons, neutrons, X-rays, α-particles, γ-rays etc.

Principle:

It is based on the principle that when charged particles or rays like α-particles, X-rays, γ-rays falls on certain materials, then these materials produces flashes of light called "scintillations". These materials are called "scintillators".

Construction and Working:

A scintillation detector consists of three components namely Scintillation crystal, Photomultiplier tube and Electronic circuitry.

1) **Scintillation detector/crystal:**

   Scintillators are available in many forms. Some commonly used scintillators are
   Inorganic crystals:

a) **NaI (TI):**

   NaI with small amount of thallium is used for detection of gamma rays. One drawback with this crystal is that it is hygroscopic and therefore is has to be sealed in airtight containers.

b) **CsI (TI) and CsI (Na):**

   CsI is used for detection of proton and alpha particles. These crystals are non-hygroscopic and have light output compared to that of NaI (TI).

c) **LiI:**

   This crystal is used for detection of neutrons.

d) **ZnS:**

   It was the first scintillator used in nuclear physics. However, making big transparent single crystal is quite difficult.

e) **$Bi_4Ge_3O_{12}$ (BGO):**

   It is non-hygroscopic, mechanically and chemically more durable compared to NaI (TI).

Organic scintillators:

Common organic scintillators are anthracene, stilbene etc. These scintillators have very poor efficiency compared to NaI (Tl) detector. However, in these scintillators, the decay time of light produced due to ionizing radiations is much shorter than in NaI (Tl) detector.

Liquid scintillators:

In these detectors, scintillator material is dissolved in certain suitable liquid. In some applications, radioactive source is thoroughly mixed with liquid scintillator. These detectors are mostly used to count very low activities specially that of beta particles.

2) **Photomultiplier tube:**

Photomultiplier tube is extremely sensitive detector of light in the ultraviolet, visible and near-infrared. These detectors multiply signal produced by incident light by as much as 10^6 to 10^8.

Photomultipliers are constructed from a glass vacuum tube which houses a photocathode, several dynodes and an anode as shown in figure 2.1.

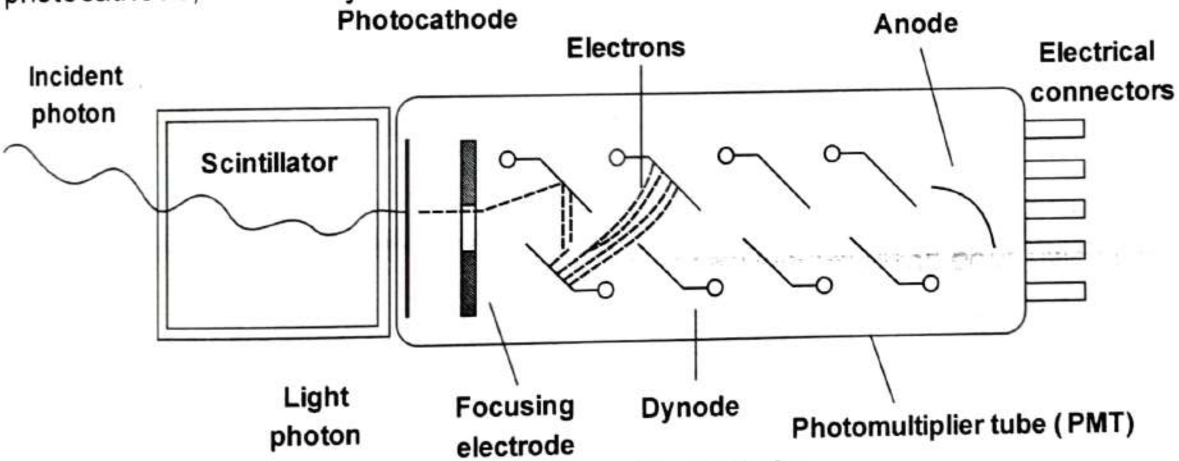

Fig. 2.1: Photomultiplier tube

Incident photons strike the photocathode of the PM tube, and electrons are produced as a consequence of the photoelectric effect. The photocathode is generally coated with either antimony-rubidium-cesium or antimony-potassium-cesium. These electrons are directed by the process of secondary emission. The electron multiplier consists of a number of electrodes called dynodes. The dynode is a plate with a surface from which electrons are easily knocked out. Each dynode is held at a more positive voltage than the previous one (50 to 100 V). The electrons are ejected by the photocathode. As they move towards the first dynode, they are accelerated by the electric field and arrive with much greater energy. On striking the first dynode, more low energy electrons are emitted and these in turn, are accelerated towards the second dynode. The process is repeated several times with the number of electrons being multiplied by three or four at each dynode. A large number of electrons reach the anode of the PMT within 10^{-6} sec. These electrons flow from the external circuit and produce a voltage pulse indicating the arrival of a photon at the photocathode. The height of voltage pulse is proportional to the energy of the incident radiation.

3) **Electronic circuitry:**

A block diagram of complete circuit is shown in figure 2.2. In this figure, the purpose of pre-amplifier is to match impedance between photomultiplier and amplifier. Amplifier amplifies the signal arriving at its input. The amplified output of the amplifier is in direct proportion to the energy deposited by rays in scintillation detector.

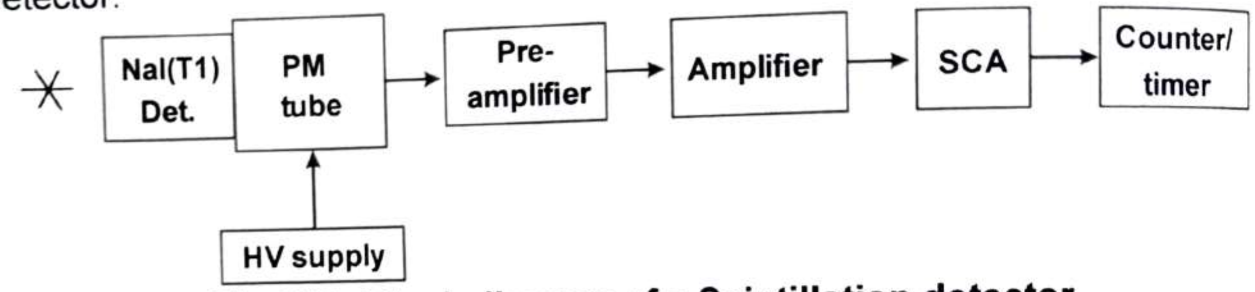

Fig. 2.2 : Block diagram of a Scintillation detector

The SCA stands for single channel analyzer. It gives the number of pulses in certain voltage interval. A typical γ-ray spectrum of ^{137}Cs emitting one γ-ray of 662KeV as shown in figure 2.3. The resolution of the scintillation detector at 662KeV is 75KeV. Similarly the γ-ray spectrum of ^{60}Co emitting two γ-rays of 1172KeV and 1332KeV as shown in figure 2.4. The two peaks are clearly visible in the spectrum.

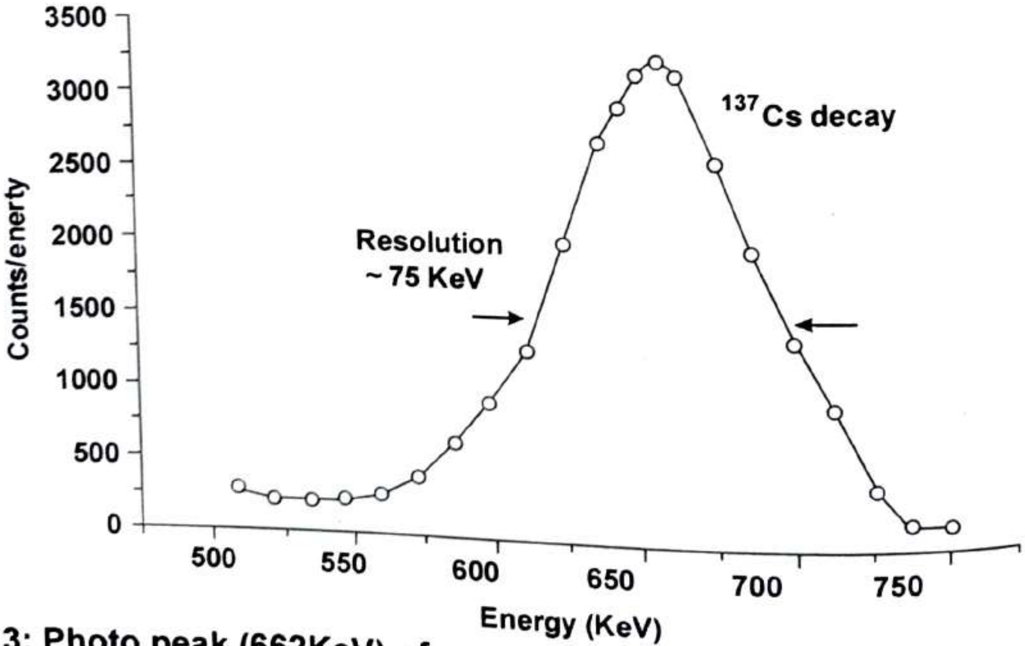

Fig. 2.3: Photo peak (662KeV) of γ-ray spectrum of ^{137}Cs as recorded by a scintillation detector. The photo peak shows an energy resolution of 75KeV.

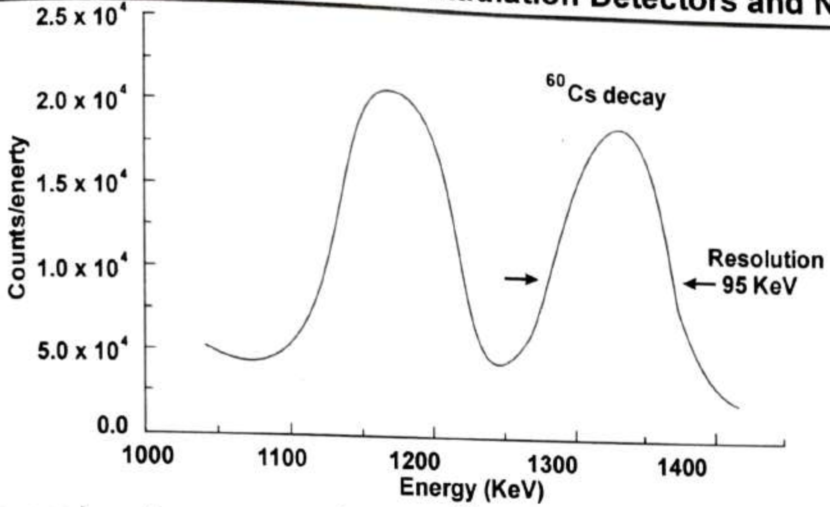

Fig. 2.4: **Photo peaks of γ-ray spectrum of ^{60}Co. It has two γ-rays of 1172KeV and 1332KeV**

Uses of Scintillation Detectors:

1) Scintillation detectors are widely used in radioactive contamination, radiation survey meters, radiometric assay, nuclear plant safety and medical imaging that are used to measure radiation.
2) There are several counters mounted on helicopters and some pickup trucks for rapid response in case of a security situation due to radioactive waste or dirty bombs.
3) Scintillation counters are designed for weighbridge applications, freight terminals, scrap metal yards, border security, contamination monitoring of nuclear waste and ports.
4) It is widely used in screening technologies, In-Vivo and ELISA alternative technologies, cancer research, epigenetics and cellular research.
5) Inorganic scintillation detectors are used to measure the energy of X-rays and γ-rays.
6) Organic scintillation detectors are used to detect β and α-particles.
7) They are rugged and can with mechanical jerks.
8) They generally have high efficiency. Efficiency is nearly 100% in case of NaI (TI) detectors.
9) They have very short dead time (~10^{-9} sec) permitting very high counting rates.

Limitations of Scintillation Detectors:

1) Energy resolution of these detectors is poor. For example, in case of NaI (TI) detector, the energy resolution is 8-10% at 662KeV.
2) The NaI (TI) detector is hygroscopic. If it absorbs moisture, it is completely damaged.

Question: Why sodium iodide crystal is doped with thallium in NaI (TI) scintillation detector?

Answer: The emission spectrum of pure sodium iodide (NaI) has maxima at a wavelength of 303nm. Most of the photomultiplier tubes are not sensitive to this wavelength. Addition of a small quantity of thallium (0.1 to 0.5% mole fraction of Tl) shifts this wavelength to 410nm. Most of the photomultiplier tubes are sensitive to this wavelength. So, Tl in scintillators is known as wavelength shifter. Also, the doping of the NaI crystal with Tl improves the scintillation efficiency by improving the light emission due to the improved recombination by the light emission of electrons and holes at the dopant site.

2.2.2 Semiconductor Detector :

The field of nuclear physics has been completely revolutionized with the development of semiconductor radiation detectors. A semiconductor detector is a solid state version of gaseous ionization chamber. It is simply a reverse biased p-n junction diode. In these diodes, ionizing radiations produce electron-hole pairs in the depletion region. This process is just like creation of electron-ion pairs in ionization chamber. These pairs are collected by the electric field applied and thus detector gives an electric pulse. The amplitude of this pulse is proportional to the energy of ionizing radiations. Since semiconductor detector is a reverse biased, therefore the signal is much larger than the noise due to leakage current.

The electronic structure of semiconductors is such that, at ordinary temperatures, nearly all electrons are tied to specific sites in the crystalline lattice and are occupying the valence band. At any given time, a few electrons gain sufficient thermal energy to break loose from localized sites in the valence band and shift to conduction band and are called conduction electrons. Since some energy must be expended in freeing an electron from its normal place in the covalent lattice of a crystal as there is a band gap that separates bound valence electrons from free conduction electrons as shown in figure 2.5.

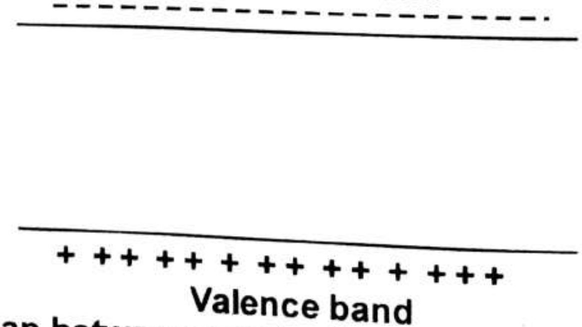

Fig. 2.5: Energy gap between conduction and valence band for silicon.

In pure crystals, no electrons can have energy within this gap. In silicon, the band gap is about 1.1eV and in germanium it is about 0.7eV. In perfect materials held at absolute zero temperature, all electrons are theoretically bound to specific lattice sites, so that the valence band is completely filled and the conduction band is empty. The thermal energy available at ordinary temperatures allows some electrons to be freed from specific sites and be elevated across the band gap to the conduction band. Therefore, for each conduction electron that exists, an electron is missing from a normally occupied valence site. This electron vacancy is called a hole, and in many ways it behaves as though it is a point positive charge. If an electron jumps from a nearby band to fill the vacancy, the hole can be thought of as moving in the opposite direction. Both electrons in the conduction band holes in the valence band can be made to drift in a preferred direction under the influence of an electric field.

In semiconductor detectors, an electric field is present throughout the active volume, i.e. the volume of the detector or total volume of the depletion region where incident radiations are detected. Semiconductor detectors offers many advantages over scintillation or gas filled detectors.

Advantages :

1) Excellent energy resolution.
2) Linear response over wide-energy range of incident radiation.
3) These detectors are generally compact and are small in size.
4) These detectors are fast detectors.
5) These detectors can be fabricated in a wide range of sensitive depth and geometry.

Initially, these detectors were developed for detection of heavy charged particles. Later on, with the advancement in semiconductor technology, detectors were developed for detection of electrons, X-ray and γ-rays. Let us discuss some semiconductor detectors.

2.2.3 Si (Li) and Ge (Li) Detectors :

Silicon Lithium Si (Li) Detectors :

Till 1968, the techniques available could not reduce the impurity concentration in silicon to less than about 10^{12} atoms/cc. With these impurity concentrations, it was not possible to fabricate a good semiconductor detector. This situation was overcome by using special techniques. One such commonly used technique is to begin with p-type silicon and diffuse into its surface Li atoms, which is tend to act as donor atoms and this creates a thin n-type region. This p-n junction is now put under reverse bias of about 500V and at a slightly higher temperature (~120°C). This causes the Li to drift into the p-type region, making a quite thick (3-5 mm) depletion region. Such a detector is known as Si (Li) (called as sili) detector. These detectors must be kept at liquid nitrogen temperature (-196°C or 77K), otherwise the Li will migrate out of its lattice sites, destroying the effectiveness of the detector. Keeping the detector at liquid nitrogen temperature also reduces the background electrical noise in the detector.

Si (Li) detectors are mostly used for measuring energy of X-rays. They offer excellent energy resolution in the X-ray region. Typical energy resolution of these detectors is of the order of 160-180eV for 5.9KeV X-rays from ^{55}Fe. A typical X-ray spectrum of ^{55}Fe recorded with the Si (Li) detector is shown in figure 2.6. The energy resolution of this detector is 180eV at 5.9KeV.

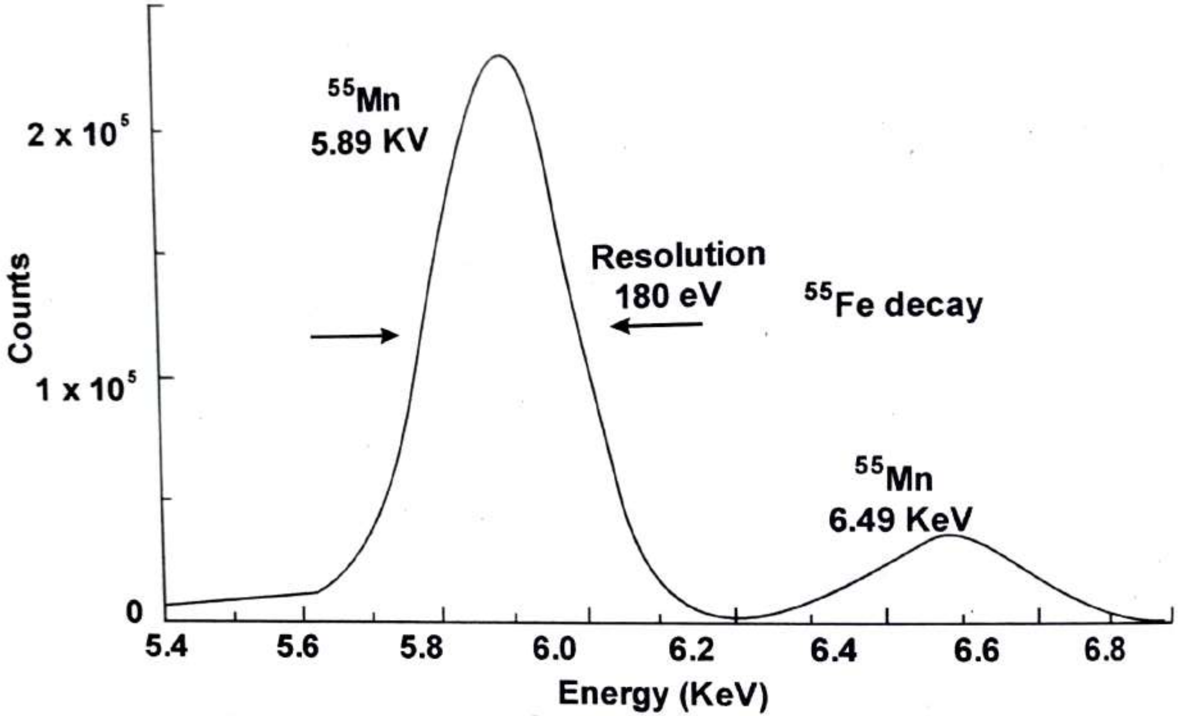

Fig. 2.6 : X-ray spectrum of ^{55}Fe as recorded by Si (Li) detector.

Germanium Lithium Ge (Li) Detectors:

The photoelectric cross-section varies as Z^5, therefore germanium is a better detector for high energy gamma rays compared to silicon detector. The method of fabrication of Ge (Li) detector is similar to that of Si (Li) detector. In Ge (Li) detectors large active volume (i.e. total volume of the depletion region) has been obtained like Si (Li) detectors. Ge (Li) detectors with active volume of 5cc to 100cc are commonly available. Like Si (Li) detectors, Ge (Li) detectors are always maintained at the liquid nitrogen temperature, while in use or when they are stored. If by mistake, Ge (Li) detector comes to room temperature, then due to migration of Li, the detector is permanently damaged. The energy resolution of Ge (Li) detector is ~1.8KeV for 1332KeV ^{60}Co γ-ray.

The typical spectrum of ^{60}Co is shown in figure 2.7. In order to visualize the comparative energy resolution of Ge (Li) and NaI (Tl) detectors, γ-ray spectrum from both these detectors under similar conditions is shown in figure 2.8. The energy resolution of the Ge (Li) detector is about 2KeV whereas for NaI (Tl) detector it is about 70KeV.

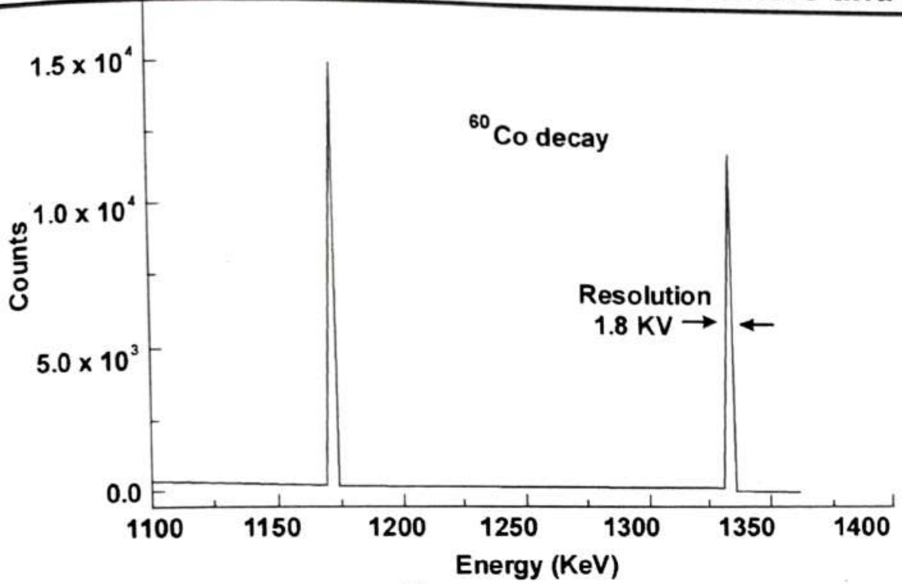

Fig. 2.7 : γ-ray spectrum of ^{60}Co as recorded by Ge (Li) detector

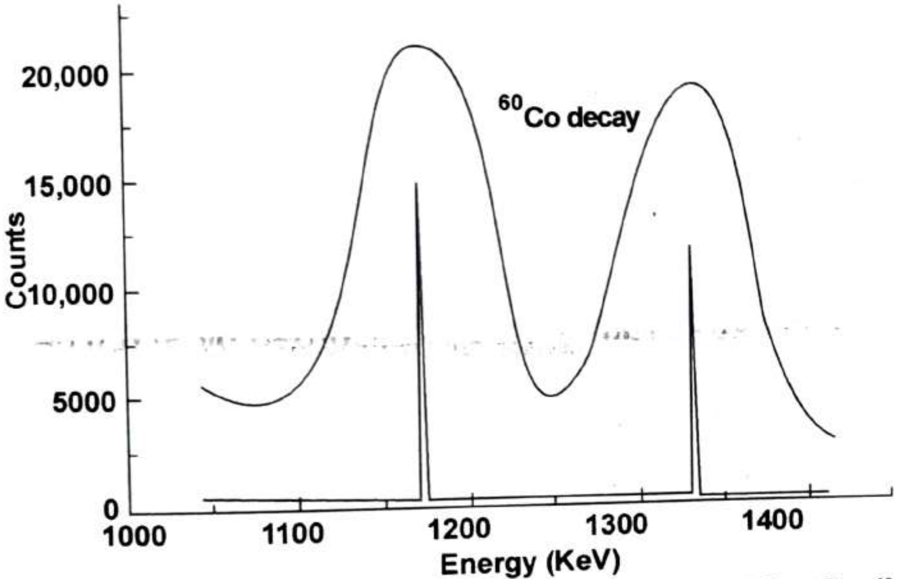

Fig. 2.8 : Comparative γ-ray spectrum of ^{60}Co as recorded by Ge (Li) and NaI (Tl) detectors

2.2.4 High Purity Germanium (HPGe) Detector :

With the advancement of semiconductor technology, it became possible to get germanium of very high purity, i.e. about 1 atom of impurity for about 10^{13} to 10^{14} atoms of germanium. Because of this high purity, it has become possible to fabricate thick detectors without lithium compensation. These germanium detectors are commonly referred as High Purity Germanium (HPGe) detectors. The biggest advantage of this is that the HPGe detectors can be maintained or stored at room temperature. There is no lithium in these detectors. However, HPGe detectors like Si (Li) or Ge (Li) detectors must be operated at liquid nitrogen temperature. Keeping the detector at liquid nitrogen temperature reduces the background electrical noise generated in the detector due to thermal energy. The energy resolution of this detector is 1.8KeV at 1332KeV. Like Ge

(Li) detectors, these detectors are also commonly available with active volume of 5cc to 100cc.

2.2.5 Cloud Chamber :

It is one of the detectors, which provides visual trajectory of a charged particle like electron, proton, α-particles, etc. Cloud chamber is also known as Wilson Cloud Chamber was built by C.T.R. Wilson in 1911.

Principle:

It is based on the principle that when dust-free air saturated with vapours of a liquid (like water, alcohol, ether, etc.) is allowed to expand adiabatically, super-saturation occurs. If at this stage an ionizing particle enters the chamber and creates ion-pairs, tiny droplets of liquid condense on these ions and form a visible track along the path of the ionizing radiation. These visible tracks can be photographed. In some cases, cloud chamber is subjected to a strong magnetic or electric field. Such a field causes the charged particles to travel in curved path. The curvature of the curved path gives information about the mass and charge of the ionizing particle.

Construction:

A simplified form of a cloud chamber is shown in figure 2.9. It consists of a transparent cylindrical chamber CC in which piston P is fitted at the bottom. On the top of this cylindrical chamber is an optically-flat glass plate G and a camera from the top views inside the chamber. This chamber is illuminated from a side with the help of a strong light source.

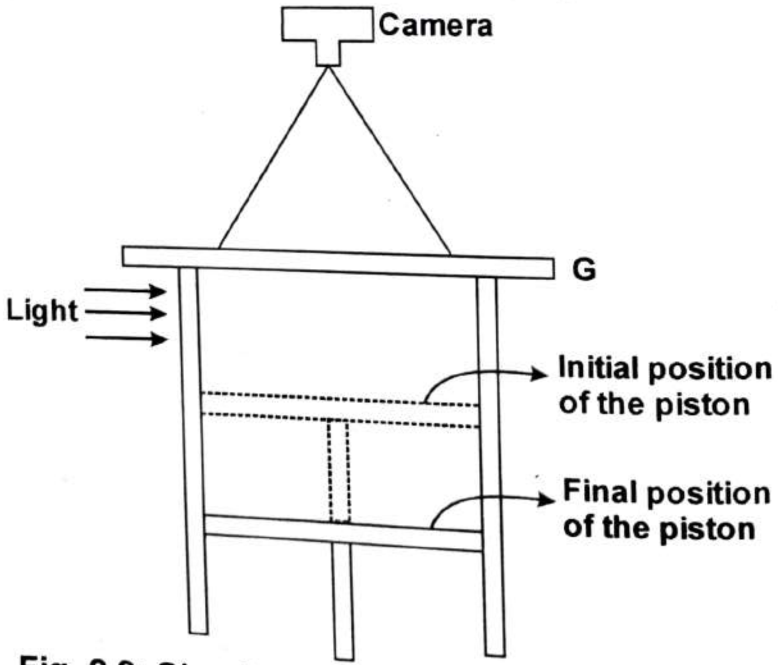

Fig. 2.9: Simplified diagram of cloud chamber

Working:

Air saturated with given liquid is filled in the space between movable piston P and glass plate G. The pressure inside the chamber is kept high. The pressure in the chamber is lowered by moving the piston down suddenly due to which the temperature of the saturated liquid falls and vapours become super-saturated. If at this moment, a charged particle passes through the chamber, it will produce ion-pairs. The super-saturated vapours condense on the ions and a trail of droplets along the path of the charged particle is seen. These tracks are known as cloud tracks. These tracks have distinctive shapes. For example, an α-particle track is broad and straight while an electron's trajectory is thinner and shows a zigzag trajectory. If the chamber is illuminated with light, a camera can take a photograph of the track, which appears as a white line on a dark background. When a vertical magnetic field is applied, positively and negatively charged particles curve in opposite directions.

Advantages:

1) When subjected to electric or magnetic field, cloud chamber is used to find charge on the ionizing particles and their momentum.
2) With cloud chamber, the range of high energy particles can easily be determined.
3) By seeing the broadness of a cloud track, we can immediately get an idea whether the track is due to heavy particle like α-particle or light particle like electron.

Limitations:

1) If the energy of the ionizing particle is high, it may not completely stop in the cloud chamber and may come out of the chamber. So, we will not get full information about the particle.
2) The recovery time of the cloud chamber is relatively very long, 10-60 sec after the expansion, so it may miss many ionizing particles.

2.2.6 Bubble Chamber :

The basic drawback of cloud chamber is that because of the low density of the gas, it is not possible to observe high energy particles. In 1952, D.A. Glaser at the University of Michigan, conceived the idea of using superheated liquid to display the tracks of ionizing particles, just as a cloud chamber utilizes a super-saturated vapour. The instrument based on this concept is known as a Bubble Chamber, because the tracks in bubble chamber consists of closely spaced bubbles, whereas in a cloud chamber there are tiny droplets of the liquid.

Principle:

It is based on the principle that under high pressure it is possible to heat a liquid without bubble formation well above its normal boiling point. If suddenly pressure is released, the liquid remains in a superheated state for some time. If such a superheated liquid is exposed to ionizing particles, the ionizing particles produce ion-pairs and these ions act as condensation centers for the formation of vapour bubbles along the path of the particle.

Construction:

The schematic diagram of the bubble chamber is shown in figure 2.10.

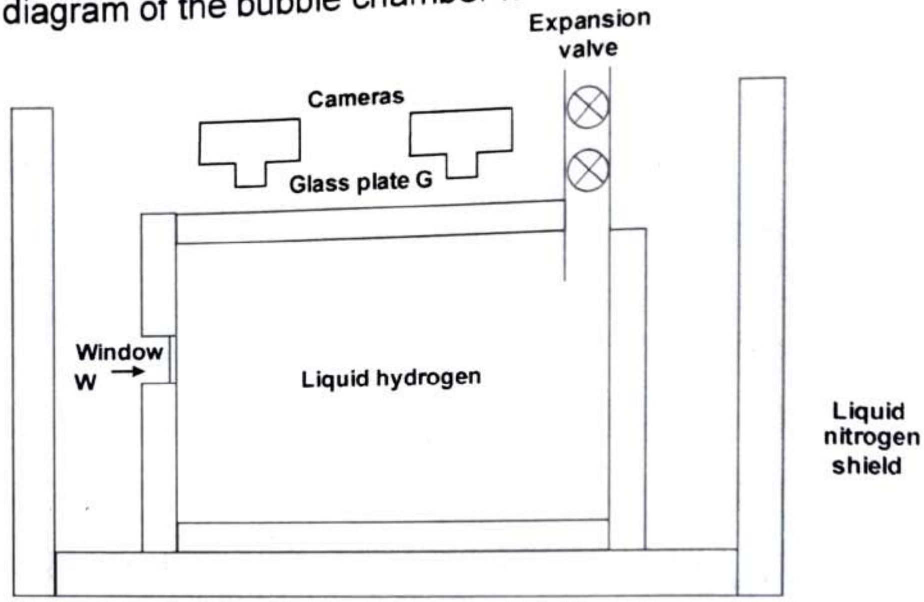

Fig. 2.10 : Schematic diagram of bubble chamber

The main body of the chamber is made up of stainless steel with thick glass ports at the top for a viewing camera. A box of thick-walled glass is filled with liquid hydrogen and is connected to the expansion pressure system. In order to maintain the chamber at constant temperature, it is surrounded by liquid nitrogen. High energy particles are allowed to enter the chamber from a side window W.

Working:

Initially, the liquid hydrogen is kept under high pressure, but when a charged particle is passing through it, the pressure is released so that the liquid is in superheated state. The liquid vapours get condensed in the form of bubbles on the ions formed by ionizing particle and photographs of the tracks formed are obtained by the cameras. Generally, bubble chamber is subjected to a strong magnetic field in order to distinguish the sign of the charge on the ionizing particles and to measure their momenta from the radius of curvature of the bubble tracks. Though most commonly used liquid in bubble chamber is liquid hydrogen, other liquids such as deuterium, helium, xenon, propane, pentane, etc. also used in some cases.

Advantages:

1) Due to high density of the liquid, even high energy cosmic rays can also be recorded in bubble chamber.
2) The bubble chamber is sensitive to both high and low ionizing particles.
3) As bubbles grow rapidly, the tracks formed in bubble chamber are clean and undistorted.

Limitations:

1) The time during which bubble chamber is sensitive is only few milliseconds, the entry of ionizing particles and photographing the tracks formed must take place during this short time.

2) Bubble chambers are the costliest detectors.

2.2.7 Spark Chamber :

It is also an image forming detector. The details of a spark chamber are as under.

Principle:

A high voltage is maintained between two parallel plate electrodes in a gas. However, the electric field between the plates is not strong enough to permit the passage of spark. Now, if an ionizing particle enters the gas, it ionizes the gas atoms creating ion-pairs along its trajectory. This provides a low resistance path and due to high voltage across the electrodes a spark takes place along the trajectory followed by the ionizing particle.

Construction:

Spark chamber consists of parallel plates of conducting material like aluminium spaced from about 0.2cm to 3cm apart. The number of plates may range from a few to a hundred or more depending upon the nature and purpose of the experiment. The size of the plates can be as large as several square feet in area. Alternate plates are connected to a high voltage direct pulse generator so that electric field of the order of 10,000 to 15,000 volts/cm can be applied between adjacent pair of plates. The spark chamber is generally filled with neon or argon or a mixture of 90% neon and 10% helium. The schematic diagram of spark chamber is shown in figure 2.11.

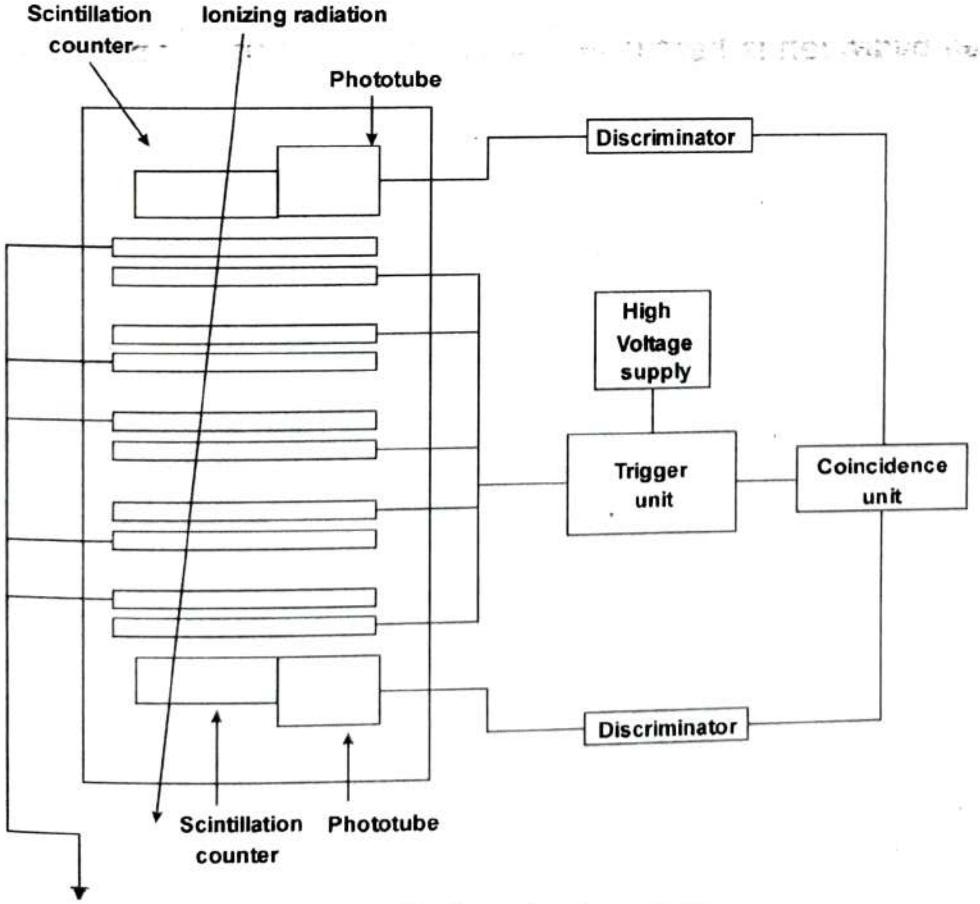

Fig. 2.11: Spark chamber

Working:

When a high energy particle enters the spark chamber, the scintillation detector outside the chamber sends a pulse to the high voltage pulse generator, which in turn sends a high voltage pulse to the spark chamber plates. When a high energy charged particle passes through the chamber, it produces large number of ion-pairs along its path. A visible spark jumps along the path of the ionizing particle between two plates. Camera records the visible track of the particle.

Advantages:

1) It is capable of fast operations.
2) It provides good definition of direction of the ionizing particles.
3) It is relatively cheaper compared to bubble and cloud chambers.

Limitation:

Spark scatter 15 to 20 thousandths of an inch, and the path uncertainty increases as the path of the particle becomes parallel to the plates.

2.3 Nuclear Models :

A good nuclear model must satisfy following two criteria.

1) It must reasonably well account for previously measured nuclear properties.
2) It must predict additional nuclear properties that can be measured in new experiments.

Let us discuss some nuclear models in detail.

2.3.1 Liquid Drop Model :

This model makes comparison between nucleus of an atom and a drop of a liquid. Nucleus is very small quantum particle. This is the central core of an atom. A drop of liquid is a macroscopic collection of molecules. By assuming nucleus to behave like a drop of liquid, we can make very accurate predictions of some of the properties of the nucleus.

Similarities between nucleus and a drop of liquid

1) Both the nucleus and a drop of liquid contain large number of particles.
2) Both the nucleus and a drop of liquid are homogeneous and incompressible.
3) The nuclear mass density is constant throughout its entire volume and drops to zero near its boundary surface just like a liquid drop.

4) In a nucleus, nucleons interacts strongly only within its nearest neighboring nucleons. It is similar to a drop of liquid in which the molecules only interacts with its neighboring molecules.

5) Both a drop of liquid and nucleus shows surface tension effect. Because of this nucleus, just like a drop of liquid tends to be spherical in shape in absence of other forces.

6) Binding energy of the nucleus is analogous to heat of vaporization of liquid. That is, evaporation of molecules from a liquid drop is similar to loss of nucleons from a nucleus when provided external energy.

7) This similarity is related to fission and fusion. When you have drops of liquid, then they can merge together to form a larger drop of liquid and similarly a large drop of liquid can break apart and become two individual smaller separate drops of liquid. This is very much similar to fusion and fission of nuclei during nuclear reactions.

Semi-Empirical Mass Formula (Weizsacker Semi-Empirical Mass Formula)

The analogy between nucleus and liquid drop has been used to set up a semi-empirical formula for mass or binding energy of a nucleus in its ground state. The mass of the nucleus can be expressed in terms of the total binding energy B and the masses of Z protons and N neutrons as

$$M = ZM_p + NM_n - B \tag{1}$$

The binding energy B of a nucleus is given by the sum of five terms as

$$B = B_v + B_s + B_c + B_a + B_p \tag{2}$$

These terms are explained in the following sections.

1) **Volume Energy Term (B_v) :**

The volume term arises from the interactions of the nucleons through the strong force. When a liquid drop evaporates, the energy required for this process is the product of mass of the drop M_m and latent heat of vaporization L. This energy is used to break all the molecular bonds. This is same as the binding energy of the drop B. So

$$B = LM_mN \tag{3}$$

Where N is the number of molecules in the drop. Equation (3) can also be written as

$$\frac{B}{N} = LM_m = \text{constant} \tag{4}$$

This means that $\frac{B}{N}$ is independent of the number of molecules present in the liquid drop. We know that neutrons and protons are held together in nuclei by short range forces. These forces reduce the mass of the nucleus below that of its constituents by an amount proportional to the number of nucleons A. Since the volume of the nucleus is proportional to A, hence this term is regarded as a volume binding energy and in analogy to equation (4) is given by

$$B_v = a_v A \tag{5}$$

Where a_v is a proportionality constant and subscript v is for volume.

2) **Surface Energy Term (B_s) :**

This term is basically result of surface nucleons on the given nucleus. Larger the surface area of nucleus, the greater will be surface energy which tends to decrease the stability or binding energy of nucleus.

Surface area= $4\pi R^2$

But $R = R_0 A^{1/3}$

Therefore, $B_s = 4\pi {R_0}^2 A^{2/3}$

$$B_s = -a_s A^{2/3} \tag{6}$$

Negative sign shows that surface energy term is going to decrease binding energy of nuclear structure.

3) **Coulomb Energy Term (B_c) :**

Inside the nucleus, not only the strong nuclear force exists between the nucleons but there exists coulombic repulsive force between proton and proton also. That coulombic force tries to break apart the protons away from nucleus. So it is going to act against the nuclear binding energy.

If there are Z protons inside the nucleus, then number of interactions are $\frac{Z(Z-1)}{2}$.

The total work done assembling a nucleus consisting of Z protons is given by

$$W = \frac{\frac{3}{5} Z^2 e^2}{4\pi\varepsilon_0 r}$$

Where r is the radius of the nucleus.

For a single proton nucleus

$$w = \frac{\frac{3}{5} e^2}{4\pi\varepsilon_0 r}$$

For a nucleus having Z protons

$$w' = \frac{\frac{3}{5} Z e^2}{4\pi\varepsilon_0 r}$$

For a single proton nucleus no work is done against Coulomb repulsion in assembling the nucleus. Thus, the true Coulomb energy term for a nucleus containing Z protons is $W - w'$.

$$B_c = -\left[\frac{\frac{3}{5}Z^2e^2}{4\pi\varepsilon_0 r} - \frac{\frac{3}{5}Ze^2}{4\pi\varepsilon_0 r}\right]$$

$$B_c = -\frac{3}{5}\frac{Z(Z-1)e^2}{4\pi\varepsilon_0 r}$$

The negative sign indicates the repulsive term. As $R = R_0 A^{1/3}$ above equation can be written as

$$B_c = -a_c \frac{Z(Z-1)}{A^{1/3}} \tag{7}$$

4) **Asymmetry Energy Term (B_a) :**

The asymmetry term reflects the stability of nuclei with the proton and neutron numbers being approximately equal. This is a term, which depends on the neutron excess $(N - Z)$ in the nucleus and it decreases with the increasing nuclear binding energy. For very few nuclei of low Z, $N - Z = 0$ (i.e. $N = Z$) and are more stable compared to their neighbours, i.e. their binding energies are maximum. The reduction in binding energy for higher A nuclei is directly proportional to $(N - Z)^2$ or square of excess of neutrons and is inversely proportional to the mass number. So, we can write

$$B_a \propto \frac{(N - Z)^2}{A}$$

$$B_a = -a_a \frac{(A-2Z)^2}{A} \tag{8}$$

As $A = N + Z$ and a_a is constant.

5) **Pairing Energy Term (B_p) :**

Experimentally it is found that,

$$B_p = a_p A^{-3/4} \tag{9}$$

Substituting the values from equations (5), (6), (7), (8), (9) in equation (2) we get

$$B = a_v A - a_s A^{2/3} - a_c \frac{Z(Z-1)}{A^{1/3}} - a_a \frac{(A-2Z)^2}{A} + a_p A^{-3/4} \tag{10}$$

Substituting value of B from above equation (10) into equation (1) we get the semi-empirical mass formula as

$$M = ZM_p + NM_n - a_v A + a_s A^{2/3} + a_c \frac{Z(Z-1)}{A^{1/3}} + a_a \frac{(A-2Z)^2}{A} - a_p A^{-3/4} \tag{11}$$

The various constants found are

$$a_v = 15.5 \text{ MeV}$$
$$a_s = 16.8 \text{ MeV}$$
$$a_c = 0.7 \text{ MeV}$$
$$a_a = 23.0 \text{ MeV}$$
$$a_p \begin{cases} = 34 \text{ MeV} & \text{for even–even nuclei} \\ = 0 \text{ MeV} & \text{for odd } A \text{ nuclei} \\ = -34 \text{ MeV} & \text{for odd–odd nuclei} \end{cases}$$

Achievements of Liquid Drop Model :

1) It predicts the atomic masses and binding energies of various nuclei accurately.
2) It predicts emission of α and β-particles in radioactivity.
3) The theory of compound nucleus, which is based on this model, explains the basic features of the fission process.

Failures of Liquid Drop Model :

1) It fails to explain the extra stability of certain nuclei, where the numbers of protons or neutrons in the nucleus are 2, 8, 20, 28, 50, 82 or 126 (these numbers are called magic numbers).
2) It fails to explain the measured magnetic moments of many nuclei.
3) It also fails to explain the spin of nuclei.
4) It is also not successful in explaining the excited states in most of the nuclei.
5) The agreement of semi-empirical mass formula with experimentally observed masses and binding energies is poor for lighter nuclei compared to the heavy ones.

2.3.2 Shell Model :

The liquid drop model can explain the observed variation of the nuclear binding energy with mass number A and fission of heavy nuclei but could not explain various nuclear properties such as magic numbers, spin, parity, electric quadrupole moment etc. These properties would require us to consider the motion of individual nucleons in a potential well which would give rise to the existence of a nuclear shell structure similar to electronic shells in the atom. As in atomic physics, there are inert gases He, Ne, Ar, etc. of which the outermost subshells are completely filled and electrons are tightly bound. We say that these gases are stable.

In 1948, American Physicist M.G. Mayer and German Physicists J. Hans, D. Jensen showed that, if nuclei containing number of protons and neutrons matches with numbers like 2, 8, 20, 28, 50, 82, 126 etc. then they shows very high stability. The above numbers are popularly known as magic numbers. Some nuclei contain magic numbers of protons and neutrons both. They are called doubly magic numbers and show exceptionally high stability.

Evidences to show existence of shell structure within the nucleus :

1) Nuclei containing magic number of protons and neutrons show very high stability.
2) Measurements shows that, the separation energy of a neutron from a nucleus containing a magic number of neutrons is large as compared to that for a nucleus containing one more neutron. Similar in case of separation energy of a proton.
3) The number of stable isotopes of an element containing a magic number of protons is usually large as compared to those for other elements. For example, calcium with Z=20 has 6 stable isotopes compared to 3 and 5 for argon with Z=18 and titanium with Z=22 respectively.
4) The number of naturally occurring isotones with magic number of neutrons is large compared to those in the immediate neighborhood. For example, number of stable isotones at N=82 is 7 compared to 3 and 2 at N=80 and N=84 respectively.
5) The neutron capture cross section of nuclei with magic number of neutrons are usually low. Since the neutron shells are filled up in these nuclei, the probabilities of these capturing an additional neutron is small. Similarly nuclei with magic number of protons have low proton capture cross section.
6) Nuclei with magic number of neutrons or protons have their first excited states at higher energies than in case of neighborhood nuclei.
7) The stable and product of all the three natural radioactive series (Uranium series, Actinium series and Thorium series) are three isotopes of lead ($_{82}Pb^{206}$, $_{82}Pb^{207}$, $_{82}Pb^{208}$) which all have magic number Z=82 of protons.
8) The naturally occurring isotopes whose nuclei contains magic number of neutrons or protons have generally greater relative abundance. For example, the isotopes $_{38}Sr^{138}$ (N=50), $_{56}Ba^{138}$ (N=82) have relative abundance of 82.58% and 71.70% respectively.

Assumptions for shell structure of nucleus

To develop a theory of the nuclear shell structure, it is necessary to assume

1) The existence of spherically symmetric central field of force governing the motion of individual nucleons inside the nucleus.
2) The central field of force in this case is assumed to be an average field due to all the nucleons in the nucleus. So, force on a nucleon will be same as on other nucleons.
3) Protons and neutrons separately fill levels in the nucleus.

Here we will discuss the motion of a single nucleon to describe structure of nucleus, so this model is also known as single particle shell model. Schrodinger equation can describe the motion of single nucleon, but we don't know the profile of nuclear potential. Therefore we used hit and trial method for nuclear potential.

2.3.2.1 Square Well Potential :

The problem can be mathematically simplified if we assume a potential well with infinite walls as

$$V(r) = -V_0, \qquad r < r_0$$
$$= 0, \qquad r > r_0$$

The shape of the finite square well potential is shown in figure 2.12

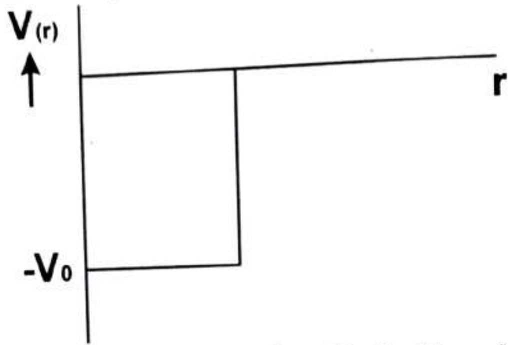

Fig. 2.12 : Square well potential. $-V_0$ is the depth of the well.

If we solve Schrodinger equation for square well potential, we get the sequence of levels as 1s, $1p, 1d, 2s, 1f, 2p, 1g, 2d, 1h, 3s, 2f, 1i, 3p, 2g$ and so on, where $s, p, d, f, g, h, i, \ldots\ldots$ etc. stand for usual spectroscopic natation $l = 0, 1, 2, 3, 4, 5, 6, \ldots..$, respectively.

Level	Number of nucleons	Magic numbers
1s	2	2
1p	6	8
1d	10	18
2s	2	20
1f	14	34
2p	6	40
1g	18	58
2d	10	68
1h	22	90
3s	2	92
2f	14	106
1i	26	132
3p	6	138

Table 2.1 : Nuclear levels and magic numbers predicted by square well potential

Because of the two different spin orientation of the nucleon, a level can contain $2(2l + 1)$ protons or neutrons. For example, number of nucleons in $1s$ $(l = 0)$ shell will be 2(2(0)+1)=2 and number of nucleons in $1f$ $(l = 3)$ shell will be 2(2(3)+1)=14. This model predicts the shell closures at nucleon number 2, 8, 18, 20, 34, 40, 58, etc. as shown in above table 2.1. The numbers shown in column 3 of the above table are not the observed magic numbers. The sequence of levels for the square well potential is shown in figure 2.13.

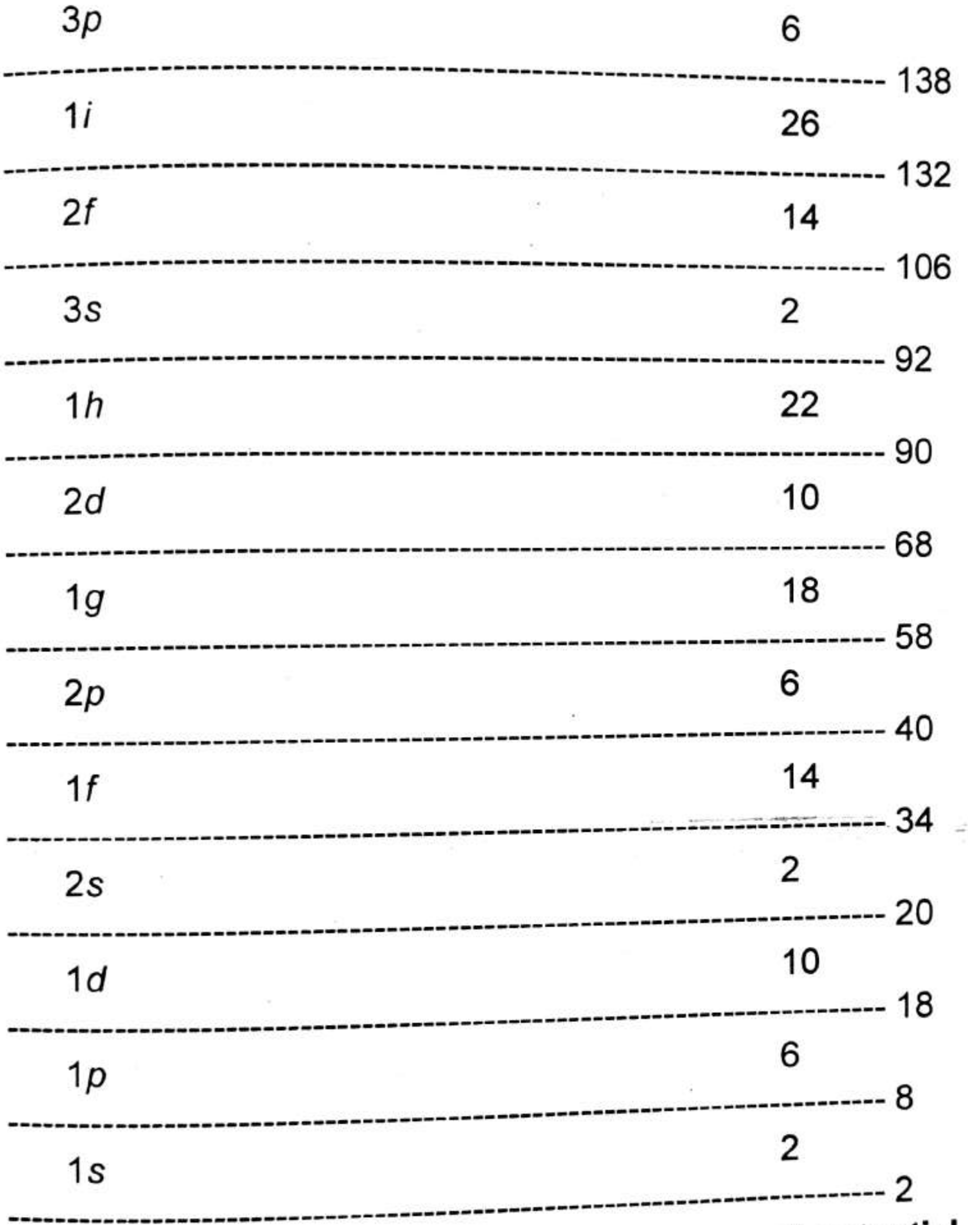

Fig. 2.13: Sequence of levels of the square well potential

The level sequence for square well potential can be remembered in the following way. First in a vertical column write the level sequence $1s, 1p, 1d, 1f, 1g, 1h, 1i$, etc. as shown in figure 2.14. Then leave two vertical spaces as blank and again write the level sequence $2s, 2p, 2d, 2f, 2g$, etc. Again leave two vertical blank spaces and write level sequence $3s, 3p, 3d, 3f$, etc. as shown in figure 2.14. In this sequence, $3s$ level will shift between $1h$ and $2f$. Similarly, $1i$ level will shift between $2f$ and $3p$ as indicated by arrow in the figure 2.14. The resulting sequence will look as shown in figure 2.15. Now, starting from the top and move horizontally from left to right, the first level is $1s$, second $1p$, third $1d$, fourth $2s$, fifth $1f$, and so on.

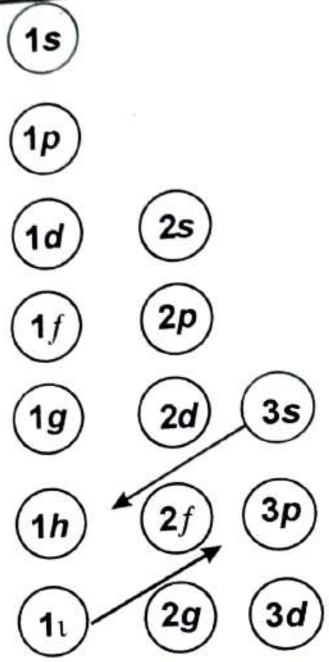

Fig. 2.14 : Way to remember the square well potential levels

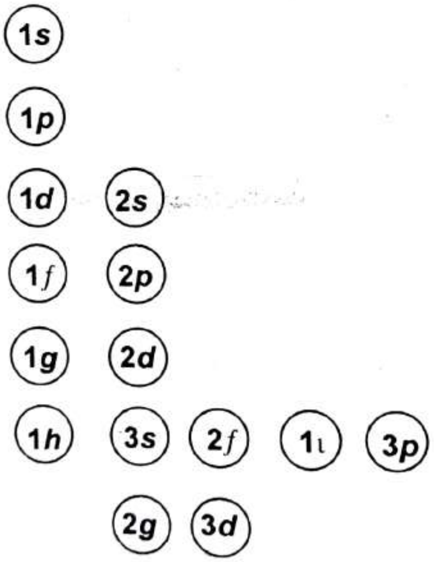

Figure 2.15: The resulting sequence is the sequence of square well potential levels

2.3.2.2 Harmonic Oscillator Potential :

Mathematical form of this potential is

$$V(r) = -V_0 + \frac{1}{2} K r^{2}$$

The shape of this potential is shown in figure 2.16. This potential and the square well potential provide two contrasting viewpoints. The square well has infinite sharp edges. The harmonic oscillator potential diminishes steadily at the edges.

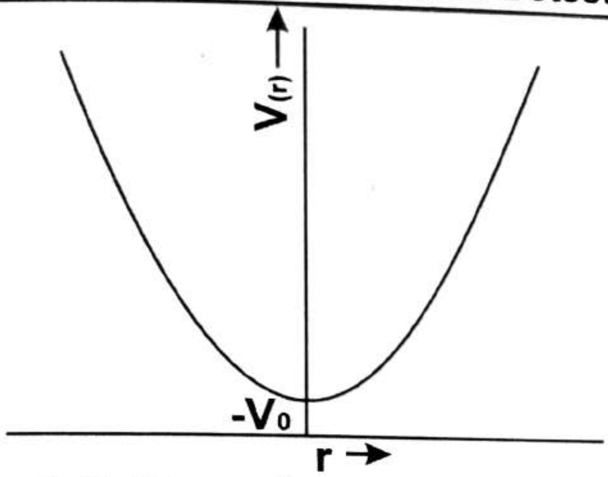

Fig. 2.16: Harmonic oscillator potential

Again solving Schrodinger equation for harmonic oscillator potential, we get the following sequence of levels as shown in first column of table 2.2. The first level is $1s$, second is $1p$, third level contains two subshells $2s$ and $1d$ having same energy, fourth level again contains two subshells $2p$ and $1f$ and so on.

Table 2.2 : Nuclear levels and magic numbers predicted by harmonic oscillator potential

Level	*No. of nucleons in various levels*	*Magic number*
$1s$	2	2
$1p$	6	8
$2s, 1d$	$2 + 10 = 12$	20
$2p, 1f$	$6 + 14 = 20$	40
$3s, 2d, 1g$	$2 + 10 + 18 = 30$	70
$3p, 2f, 1h$	$6 + 14 + 22 = 42$	112
$4s, 3d, 2g, 1i$	$2 + 10 + 18 + 26 = 56$	168

In this case also each subshell contains $2(2l+1)$ protons or neutrons. For example, in fourth shell, we have two subshells $2p$ and $1f$. For $2p$ $(l = 1)$, it contains 2(2(1)+1)=6 nucleons and $1f$ $(l = 3)$, it contains 2(2(3)+1)=14 nucleons. Total number of nucleons in fourth shell = 6+14=20. These numbers are shown in the third column of the table 2.2. This level sequence again does not reproduce experimentally observed magic numbers. The sequence of harmonic oscillator levels is shown in figure 2.17. The levels are equally spaced. Harmonic oscillator level sequence can also be remembered in almost similar way as that of square well potential as shown below.

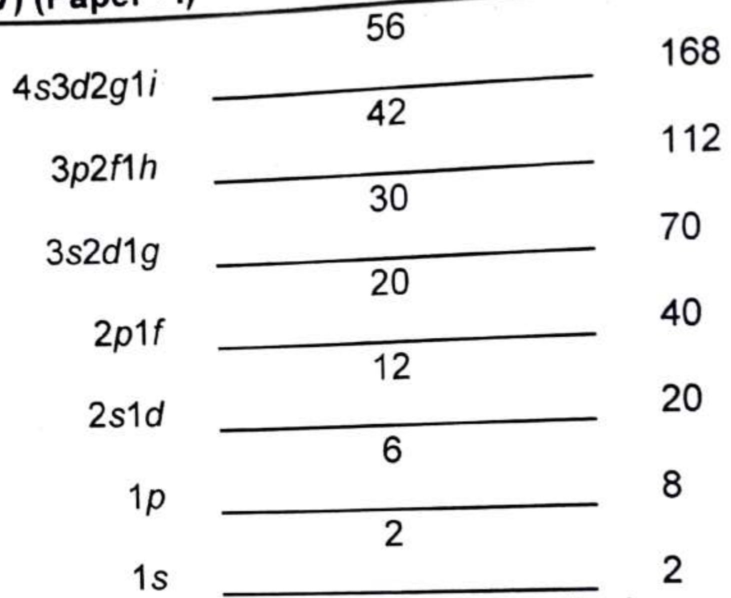

Fig. 2.17 : Level sequence as obtained for the harmonic oscillator levels

As shown in figure 2.18, write in the first vertical column the level sequence $1s, 1p, 1d, 1f, 1g, 1h, 1i$, etc. Then leave two vertical spaces as blank and again write the level sequence $2s, 2p, 2d, 2f, 2g$, etc. Again leave two vertical blank spaces and write level sequence $3s, 3p, 3d, 3f$, etc. Now these sequences read horizontally are the harmonic oscillator levels. For example, first level is $1s$, second is $1p$, third is $1d$, fourth $2s$, and so on.

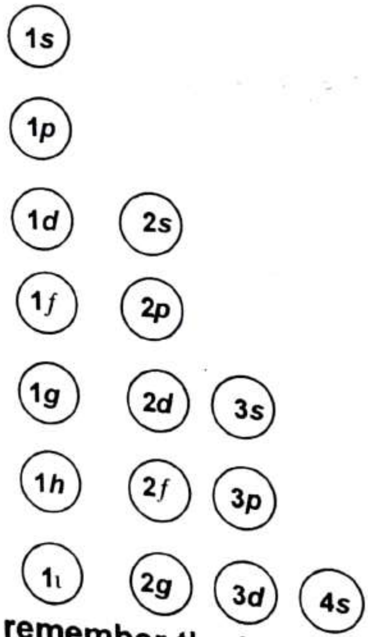

Fig. 2.18: Way to remember the harmonic oscillator levels

The other potential, which is a compromise between square well and harmonic oscillator potential, is

$$V(r) = \frac{-V_0}{1 + e^{\frac{R-r}{d}}}$$

This potential is known as Woods-Saxon potential. In this equation, $d = 0.524fm$, R is the mean radius and $r = r_0 A^{1/3}$. Unlike square well potential, the Woods-Saxon potential does not have any sharp edges at all. The harmonic oscillator potential also does not have any edges. The shape of this potential is shown in figure 2.19. This potential closely approximates the nuclear charge and matter distribution, falling smoothly to zero beyond the mean radius R. When the Schrodinger equation was solved for this potential, it predicted 2, 8, 20, 40, 58, 92, 112 as magic numbers. We again get the magic numbers 2, 8 and 20, but the higher magic numbers do not emerge from the calculations.

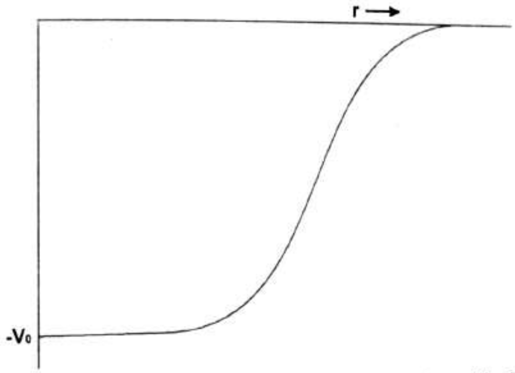

Fig. 2.19 : Wood-Saxon potential

2.3.2.3 Spin Orbit Coupling :

A way out of this difficulty, which proved to be remarkably successful was proposed independently in 1949 by M.G. Mayor in USA and O. Haxel, J.H.D. Jensen and H.F. Suess in Germany. We know that each nucleon has a spin angular momentum $s = \sqrt{s(s+1)}\,\hbar$ and orbital angular momentum $l = \sqrt{l(l+1)}\,\hbar$. It was proposed that there is a strong coupling between the orbital angular momentum and spin angular momentum of each individual nucleon referred as spin-orbit coupling. The nucleon energy level for a given value of the orbital quantum number (except $l = 0$) splits into two subshells, characterized by total angular momentum quantum number $j = l + {}^1\!/_2$ and $j = l - {}^1\!/_2$ corresponding to spin components of +1/2 and -1/2 respectively. The sign of this term is chosen in such a way that +1/2 goes down in energy whereas -1/2 goes up.

	2
$1s_{1/2}$	
	8
$1p_{3/2}, 1p_{1/2}$	
	20
$1d_{5/2}. 2s_{1/2}. 1d_{3/2}$	
	28
$1f_{7/2}$	
	50
$2p_{3/2}. 1f_{5/2}. 2p_{1/2}. 1g_{9/2}$	
	82
$1g_{7/2}, 2d_{5/2}, 2d_{3/2}. 3s_{1/2}. 1h_{11/2}$	
	126
$1h_{9/2}, 2f_{7/2}. 2f_{5/2}. 3p_{3/2}, 3p_{1/2}, 1i_{13/2}$	
	184
$2g_{9/2}. 3d_{5/2}. 1i_{11/2}. 2g_{7/2}, 4s_{1/2}, 3d_{3/2}, 1j_{15/2}$	

The sequence of these levels is shown in figure 2.20.

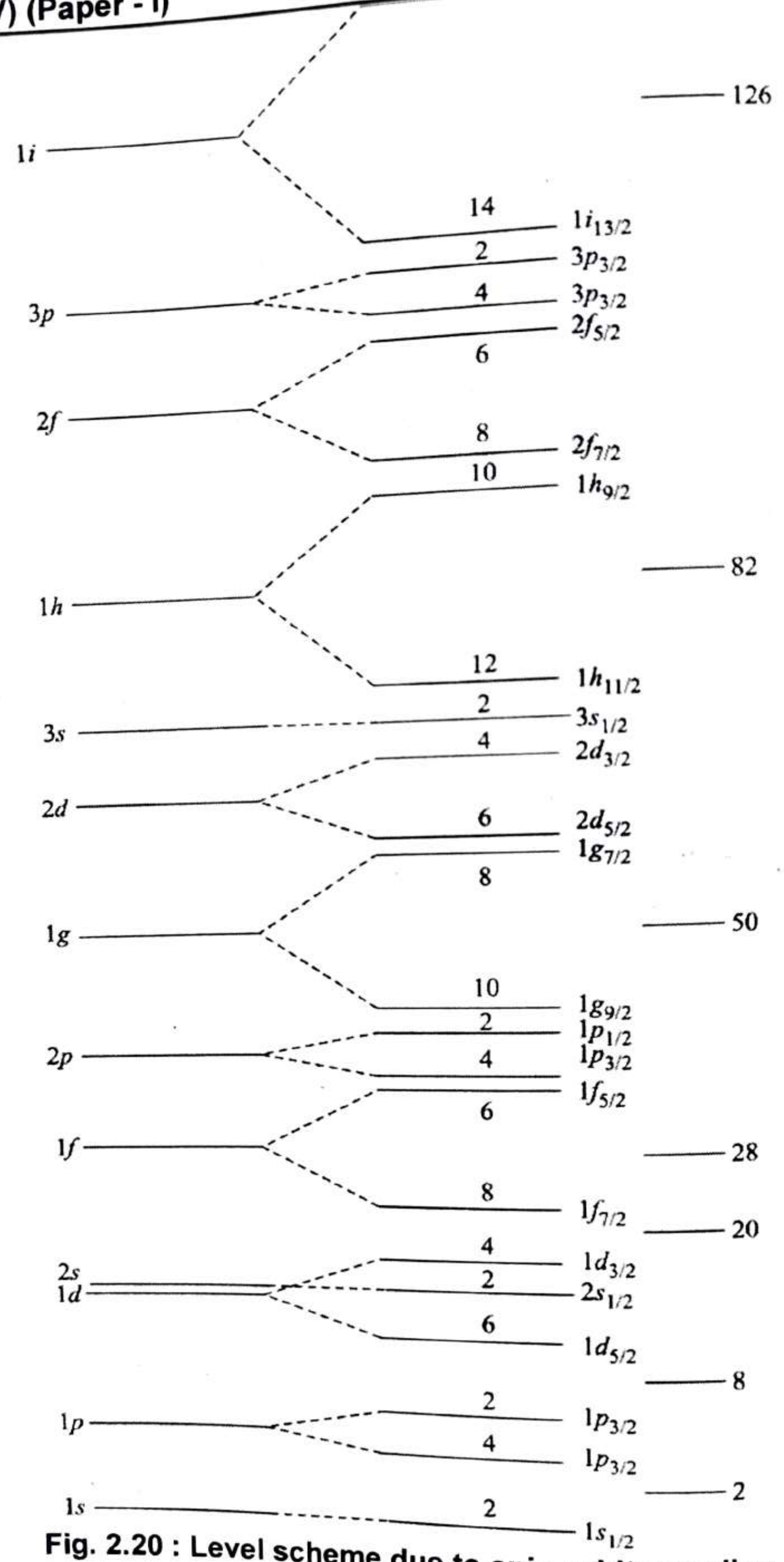

Fig. 2.20 : Level scheme due to spin-orbit coupling

2.3.2.4 Predictions of Shell Model :

1) Stability of the closed shell nuclei reproduces all the magic numbers.
2) Even-even nuclei have ground state angular momentum or spin 0. There is no known exception to this rule.
3) In odd A nuclei, the spin will be determined by the last unpaired particle.
4) An odd-odd nucleus will have a total angular momentum which is the vector sum of the odd neutron and odd proton *j* values. The parity will be the product of the proton and neutron parities.
5) In an odd nucleus, the total angular momentum *I* of the nucleus is equal to the angular momentum *j* of the last unpaired nucleon. Thus we see that magnetic moment of the nucleus is produced by the odd nucleon only.
6) The shell model also makes predictions about the electric quadrupole moment of the odd A, odd Z nuclide, on the assumption that this is due to the unpaired proton.
7) The single particle model has succeeded in explaining the phenomenon of nuclear isomerism. The shell model also predicts that almost all of the isomeric states with long life are found for nuclei with N or Z near the end of a shell.
8) Theory of beta decay shows that the life time can be understood in terms of relative parity and angular momenta of the states involved.
9) Stripping reactions can be explained by single particle model.

2.3.2.5 Achievements and Failures of Shell Model :

Achievements of Shell Model :

1) It explains the ground state spin and parities of all even-even nuclei without any exception.
2) It explains the ground state spin and parities of most odd A (even-odd or odd-even) nuclei.
3) It also explains the spin and parities of odd-odd nuclei.
4) It explains the extra stability of magic nuclei.
5) It also explains the qualitative features of magnetic dipole and electric quadrupole moments of different nuclei.
6) It is also able to explain many other properties, like nuclear isomerism of different nuclei.

Failures of Shell Model :

1) Shell model fails to explain spin values for certain nuclei.
2) Shell model is unable to explain the energy of first excited states in even-even nuclei.
3) It is unable to explain magnetic moments of some nuclei.
4) This model is also unable to explain quadrupole moments of many nuclei.

2.3.3 Fermi Gas Model :

The semi-empirical binding energy formula is based on treating the nucleus like a liquid drop. Such an analogy is an oversimplification and nucleus has many properties that can be explained more simply in terms of independent particle behaviour rather than in terms of the strong interaction picture implied by the liquid drop model. The most primitive independent particle model is obtained if the nucleus is treated as a degenerate Fermi gas of nucleons. The nucleons are assumed to move freely except for effects of the exclusion principle, throughout a sphere of radius $R = R_0A^{1/3}$, $R_0 = 1.2fm$. The situation is represented in figure 2.21 by two wells, one for neutrons and other for protons. Free neutrons and free protons, far away from the walls, have the same energy, and the zero level for the two wells is the same. The two potential wells though have slightly different shapes, mainly because of the Coulomb part, the well for protons is less deep because of the Coulomb potential by an amount E_C and externally the $1/r$ dependence of the Coulomb potential extends the range. Protons trying to enter the nucleus from the outside are repelled by the nuclear charge, they must either tunnel through barrier or have enough energy to pass over the barrier.

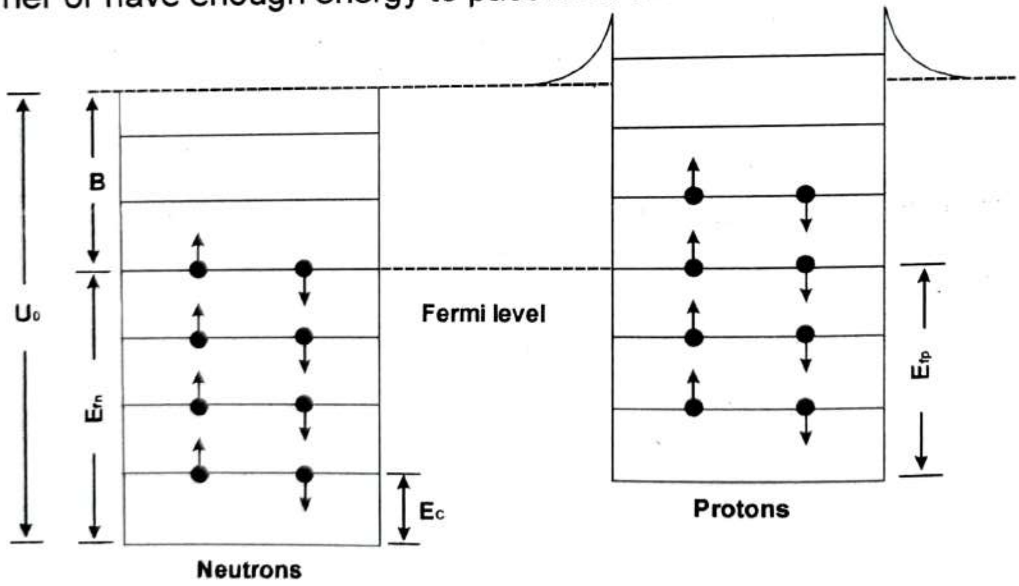

Fig. 2.21: Protons-neutron levels in Fermi model of the nucleus. The two potential wells have slightly different shapes because of the Coulomb repulsion of protons.

The wells contain a finite number of levels, each level can be occupied by two nucleons, one with spin up and other with spin down. It is assumed that the nuclear temperature is so low that the nucleons occupy the lowest states available to them. The term degenerate Fermi gas describes such a situation. The nucleons populate all states up to a maximum kinetic energy equal to the Fermi energy E_F.

From the density of the states obtained from free Fermi gas confined to stay within a volume V, the nuclear volume, the number of particle states are given by

$$n = \frac{2V}{(2\pi\hbar)^3} \int_0^{P_F} d^3P$$

Or

$$n = \frac{V{P_F}^3}{3\pi^2\hbar^3}$$

and the Fermi momentum P_F is given by

$$P_F = \hbar\left(3\pi^2\frac{n}{V}\right)^{1/3} = h\left(\frac{3}{8\pi}\frac{n}{V}\right)^{1/3}$$

Let us calculate the depth of the potential well for Z protons and N neutrons. We can write

$$P_{F,n} = \frac{\hbar}{r_0}\left(\frac{9\pi N}{4A}\right)^{1/3}$$

$$P_{F,p} = \frac{\hbar}{r_0}\left(\frac{9\pi Z}{4A}\right)^{1/3}$$

For the neutron and proton Fermi momentum respectively.

A simple estimate of the Fermi momentum can be reached by considering

$$N = Z = A/2$$

Resulting in

$$P_{F,n} = P_{F,p} = \frac{\hbar}{r_0}\left(\frac{9\pi}{8}\right)^{1/3}$$

Using the value $\hbar c = 197\ MeV\ fm$, this becomes

$$P_{F,n} \approx P_{F,p} \approx \frac{297}{r_0}\ MeV/c$$

The corresponding Fermi kinetic energy with $r_0 = 1.2fm$ becomes

$$E_F = \frac{{P_{F,n}}^2}{2m} \approx \frac{{P_{F,p}}^2}{2m} \approx 33\ MeV$$

This energy corresponds to the kinetic energy of the highest occupied orbit (smallest binding energy). The Fermi gas model gave some information about nuclear excited states even at low excitation energies observed in radioactive decay.

2.3.4 Collective Model :

The shell model has been most successful in explaining a number of nuclear features. The deviations of magnetic moments from the Schmidt curve makes this model less acceptable. The measured quadrupole moments are several times larger than can be attributed to the odd nucleon. Rainwater in 1950, suggested that these discrepancies might overcome in odd A-nuclei by considering the polarization of the even-even core by the motion of the odd nucleon. The nuclear core, consisting even nucleons, thus have a spheroidal rather than a spherical shape. This distortions would make an additional contribution to the quadrupole moment and the quadrupole transition rate. The idea of the deformed nuclear core has been developed by A. Bohr and B. Mottelson. Large nuclear quadrupole moments are found in some cases, mainly among the rare earth elements with major axis 30% larger than the minor. The mechanism by which this deformation is done been illustrated in figure 2.22.

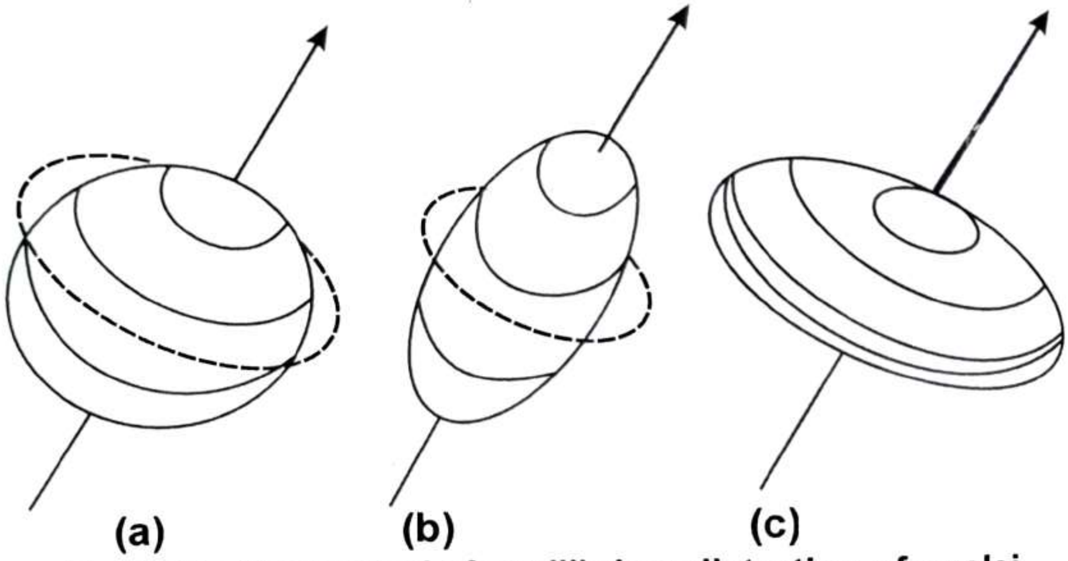
(a) (b) (c)

Fig. 2.22 : Mechanical of equilibrium distortion of nuclei

In figure 2.22 (a), a nucleon outside a closed shell is shown orbiting around a spherically shaped closed shell core. If the forces between the external nucleon and the internal core are repulsive there is a tendency to polarize the core by pushing the equatorial plane towards the center of the nucleons to form a prolate spheroid (figure 2.22 (b)). On the other hand, if the forces are attractive, polarization is accomplished by pulling out the equatorial plane to form an oblate spherical as shown in figure 2.22 (c).

The individual nucleons are imagined to move in orbits as before in a potential distribution determined by the remaining nucleons. It is suggested that the entire shell configuration can undergo periodic oscillations in shape. This collective motion of the nucleons influences the individual particle orbits because it changes the potential of the region in which these particles move. Because of the stability of the core, the collective motion is small and the independent particle characteristics are prominent, for the nuclei consisting of almost closed shells.

The scheme of nuclear energy levels which results from the collective motion of the nucleons in the core and interplay between the motions of loosely bound surface nucleons depends upon the strength of the coupling between them. When the coupling is strong, the energy states resemble with the linear molecule. The collective model does not deny the validity of the shell model. It must be realized that the individual nucleons still pursue their "quasi-interdependent" motions in a spherical potential.

According to this model, the inner core of the nucleus behaves like a non-viscous liquid drop surrounded by loosely bound nucleus in outer shell, thus combining in it the characteristics of both the liquid drop and the shell models. Nucleus has a shell structure that may oscillate in shape and size and the energy levels rise due to the collective motion of nucleus forming the core and the coupling between loosely bound nucleus and the core.

@@@@@@@@@@X0X@@@@@@@@@

Review Questions

Q. 1. **Short Answer Type Questions**

1) What is the principle and significance of a photomultiplier tube in a scintillation detector?
2) Why sodium iodide crystal is doped with thallium in NaI (TI) scintillation detector?
3) Give the properties of a good quality photomultiplier tube.
4) What are the advantages of a semiconductor detector?
5) How are the Ge (Li) detectors more suitable over the Si (Li) detectors for electromagnetic radiations?
6) What is the principle of the cloud chamber?
7) What is the principle of the bubble chamber?
8) What is the principle of the spark chamber?
9) What are the drawbacks of liquid drop model?
10) What are magic numbers?
11) Give two achievements of nuclear shell model.
12) What are the similarities between a nucleus and liquid drop?
13) State predictions of shell model.
14) List various nuclear models.
15) Name the various contributions to the binding energy of the nucleus as taken in semi-empirical formula.

Q. 2. **Long Answer Type Questions :**

1) Describe the construction and working of NaI (TI) scintillation detector.
2) What is the principle of a bubble chamber? Discuss its construction and working. What are its merits?
3) What is the principle of a cloud chamber? Discuss its construction and working. What are its merits?
4) What is the principle of a spark chamber? Discuss its construction and

working. What are its merits?

5) What is a semiconductor detector? Explain its working.

6) Write short notes on i) Cloud chamber ii) Bubble chamber iii) Spark chamber

7) Discuss the basic assumptions of liquid drop model of nucleus. Explain how the model is used to estimate the semi-empirical mass formula.

8) Derive the Coulomb energy term of semi-empirical mass formula.

9) Discuss the shell model of the nucleus. What are its merits and demerits?

10) List the experimental evidences for shell model.

11) What are the basic differences between liquid drop model and shell model of the nucleus? What is the evidence of shell structure in the nuclei? Explain the main assumptions of the shell model of the nucleus. Discuss its achievements, failures and limitations.

12) What are magic numbers? How does the shell model explain the existence of magic numbers and other nuclear properties?

13) Describe Fermi-Gas model and obtain the expression for Fermi energy of proton.

14) Write note on Si (Li) and Ge (Li) detectors.

15) Discuss the collective model of nucleus.

Reference Books

1) Introduction to Nuclear and Particle Physics by V.K. Mittal, R.C. Verma, S.C. Gupta
2) Nuclear Physics by D.C. Tayal
3) Nuclear Physics by Dr. S.N. Ghoshal
4) Nuclear Physics An Introduction by S.B. Patel
5) Nuclear Physics Principles and Applications by John Lilley
6) Nuclear and Particle Physics by K.K. Sharma, B.S. Satyal

@@@@@@@@@X0X@@@@@@@@@

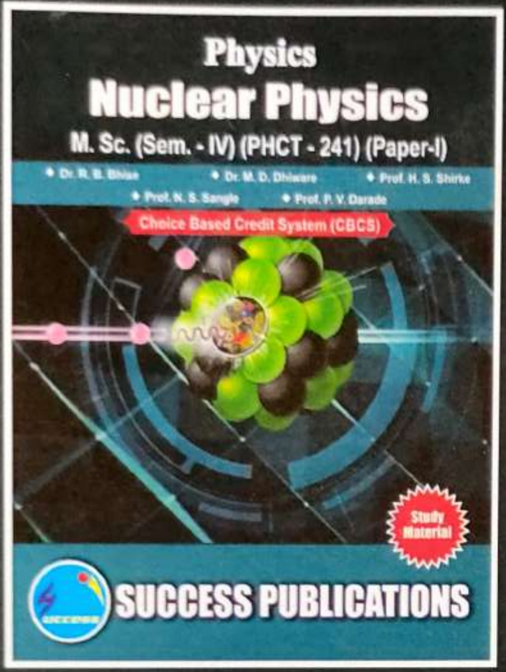

Physics

Nuclear Physics

M. Sc. (Sem. - IV) (PHCT - 241) (Paper-I)

- Dr. R. B. Bhise
- Dr. M. D. Dhiware
- Prof. H. S. Shirke
- Prof. N. S. Sangle
- Prof. P. V. Darade

Choice Based Credit System (CBCS)

Study Material

SUCCESS PUBLICATIONS

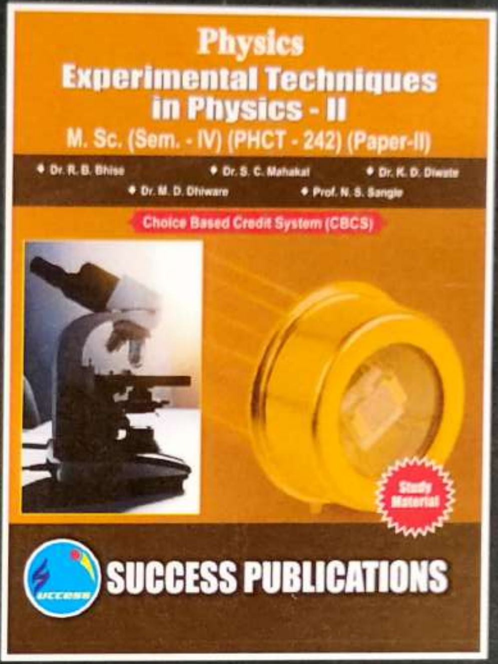

Physics

Experimental Techniques in Physics - II

M. Sc. (Sem. - IV) (PHCT - 242) (Paper-II)

- Dr. R. B. Bhise
- Dr. S. C. Mahakal
- Dr. K. D. Diwate
- Dr. M. D. Dhiware
- Prof. N. S. Sangle

Choice Based Credit System (CBCS)

Study Material

SUCCESS PUBLICATIONS

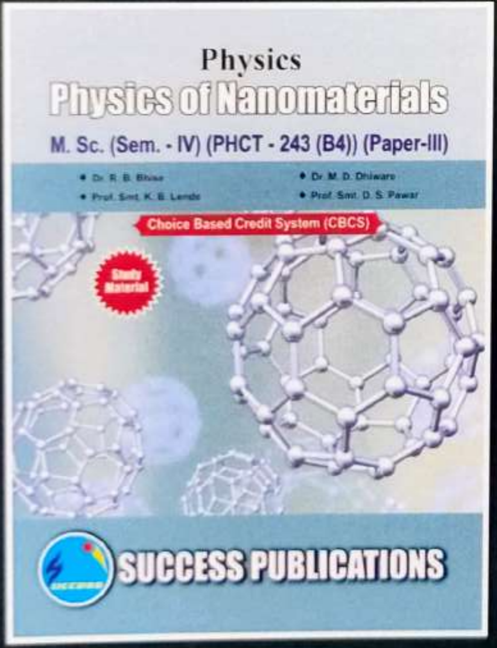

Physics

Physics of Nanomaterials

M. Sc. (Sem. - IV) (PHCT - 243 (B4)) (Paper-III)

- Dr. R. B. Bhise
- Dr. M. D. Dhiware
- Prof. Smt. K. B. Lande
- Prof. Smt. D. S. Pawar

Choice Based Credit System (CBCS)

Study Material

SUCCESS PUBLICATIONS

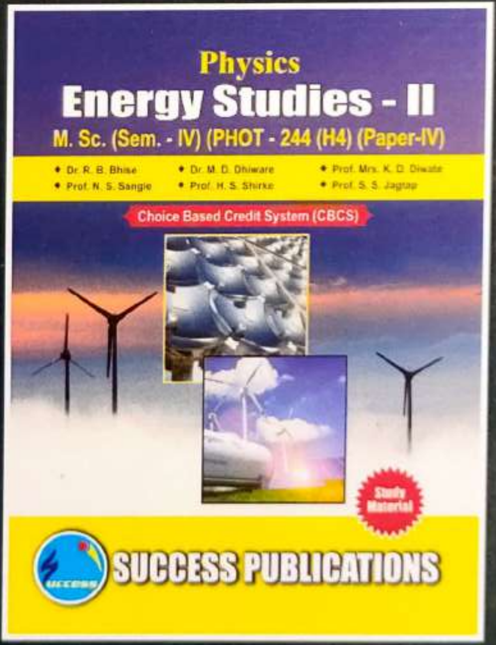

Physics

Energy Studies - II

M. Sc. (Sem. - IV) (PHOT - 244 (H4) (Paper-IV)

- Dr. R. B. Bhise
- Dr. M. D. Dhiware
- Prof. Mrs. K. D. Diwate
- Prof. N. S. Sangle
- Prof. H. S. Shirke
- Prof. S. S. Jagtap

Choice Based Credit System (CBCS)

Study Material

SUCCESS PUBLICATIONS

ISBN : 978-93-24457-46-9

SUCCESS PUBLICATIONS

PT-3841

Address : Radha Krishna Apartment, 535, Shaniwar Peth,
Appa Balwant Chowk, Opp. Prabhat Theatre, Pune - 30.
Ph. No. 24434662, Mobile : 9325315464
E-mail : sharpgroup31@rediffmail.com
Website : www.sharpmultinational.com